2-3 μm mid-infrared luminescence of Ho3(+)/Yb(3+) co-doped chloride-modified fluorotellurite glass

Dingchen Tang, Ying Tian, Dominik Dorosz, Xu Wang, Xueying Yang, Yongyan Liu, Xianghua Zhang, Junjie Zhang, Shiqing Xu

2-3μm mid-infrared luminescence of Ho^{3+}/Yb^{3+} co-doped chloride-modified fluorotellurite glass

Dingchen Tang[a], Ying Tian[a,*], Dominik Dorosz[b], Xu Wang[a], Xueying Yang[a], Yongyan Liu[a], Xianghua Zhang[c], Junjie Zhang[a], Shiqing Xu[a,*]

[a]Key Laboratory of Rare Earth Optoelectronic Materials and Devices of Zhejiang Province, Institute of Optoelectronic Materials and Devices, China Jiliang University, Hangzhou 310018, People's Republic of China

[b]Faculty of Materials Science and Ceramics, AGH University of Science and Technology, 30 Mickiewicza Av., 30-059 Krakow, Poland

[c]ISCR (Institut des Sciences Chimiques de Rennes) UMR 6226, Univ Rennes, CNRS, F35000 Rennes, France

Abstract

In this paper, Ho^{3+}/Yb^{3+} co-doped chloride-modified fluorotellurite glasses with 2-3 μm mid-infrared luminescence are prepared. By measuring and investigating the transmission spectra and emission spectra, the prepared glasses show a high transmittance (91%) and low maximum phonon energy (813cm^{-1}). Based on the measured absorption spectra, the Judd-Ofelt parameters and radiation characteristics were calculated in depth. In addition, with the assistance of phonons, the energy transfer between Ho^{3+}/Yb^{3+} ions further increases the mid-infrared fluorescence intensity. The calculated emission cross-section at 2.0μm and 2.85μm reach 16.47×10^{-21} cm^2 and 7.8×10^{-21} cm^2, respectively. It is worth mentioning that the quantum efficiencies of Ho^{3+}: $^5I_7\rightarrow{}^5I_8$ and $^5I_6\rightarrow{}^5I_7$ reach 51.47% and 84.14% respectively. The results having also in mind good thermal stability (ΔT=102℃) and refractive index (n=1.645) indicate that this glass has a promising application for the study of fiber lasers in the mid-infrared band.

Keywords

Mid-infrared fluorescence; Maximum phonon energy; Quantum efficiency; Chloride-modified fluorotellurite glass

Introduction

In recent years, luminescence in the mid-infrared band of 2-3 μm has attracted a lot of attention from researchers due to its potential applications in various aspects in remote sensing, LIDAR, human eye safety, and military [1-7]. Fiber lasers offer stable lasing while keeping the possibility of power scaling, high beam quality factor M^2=1.1 and compact structure. It makes that rare-earth-doped glass fibers have been widely investigated to obtain efficient luminescence in mid-infrared lasers.

Trivalent rare-earth ions, such as Ho^{3+}, Er^{3+}, and Tm^{3+} can be used as active ions to achieve emission wavelengths in the mid-infrared region [8-16]. Ho^{3+} ion is one of the most attractive for emission in the 2-3 μm range. Unfortunately, Ho^{3+} is limited by effective excitation among commercial high-power laser diodes, which lacks a suitable absorption band for Ho^{3+}. Effective mid-infrared luminescence can be achieved by introducing a sensitizer that absorbs pump light energy and then transferring it to donor like Ho^{3+}, where the sensitizers include Tm^{3+} or Yb^{3+} [17]. There are two reasons for using Yb^{3+} as a sensitizer in this study. On one hand, Yb^{3+} has a high absorption cross-section at 976 nm, which is a wavelength readily available for high-power single-

* Corresponding authors.
E-mail addresses: tianying0204@163.com (Y. Tian), sxucjlu@163.com (S. Xu).

mode laser diodes. On the other hand, the energy level of Yb^{3+}: $^5F_{5/2}$ is close to that of Ho^{3+}: $^5I_6$, so the pump energy absorbed by Yb^{3+} can be transferred to Ho^{3+}. Therefore, Yb^{3+} is used as a donor in the Yb^{3+}/Ho^{3+} doped system to achieve efficient excitation by the pumped LD source. The choice of the glass for a particular REs is another important factor in obtaining effective mid-infrared emission as the phonon energy of the host material determines the quantum efficiency of radiative transition [17, 18]. Fluoride and sulfur-based glasses are often used as matrix materials due to their low phonon energy, which can effectively reduce the probability of non-radiative transitions [19]. However, in majority they possess poor physicochemical stability and mechanical strength which is in contrast to heavy metal oxide glasses. In result they are often proposed as a main host material in the 2-3 μm spectral range. Among the various oxide glasses, tellurite glasses are known for their low phonon energy (750cm^{-1}), high rare earth ion solubility, high refractive index (2.0) and wide transmittance range from the visible to mid-infrared [20, 21]. Moreover, previous studies have shown that the addition of fluoride ions can change the ligand field structure of the glass and reduce the content of residual hydroxyl groups, which will facilitate the improvement of the NIR transmittance edge of tellurite glasses and enhance the luminescence of rare-earth emission at 3 μm [22]. In recent years, a large number of studies on the thermal stability, structural and optical properties of fluoride and fluorotellurite glasses have been reported in the literature [23, 24]. In order to improve the luminescence properties of fluorotellurite glass, it is found that the introduction of Cl^- could not only enhance the thermal stability of glass, but also improve the luminescence efficiency [25]. So far, there are few reports on chloride-modified Ho^{3+}/Yb^{3+} co-doped fluorotellurite glass systems, so there are no complete and specific studies on thermal stability and structural analysis, as well as systematic studies on the effect of chloride content on spectral properties. This study aims to accomplish this task presenting investigation on chloride-modified fluorotellurite glasses prepared by a high-temperature melting method. Subsequently, the infrared transmittance and thermal stability of the samples were tested and studied in comparison. It was found that the thermal stability of the glass was enhanced with the increase of chloride content after the introduction of chloride and the hydroxyl content was reduced to some extent. The highly efficient mid-infrared luminescence is achieved by the chloride-modified fluorotellurite glass based on low phonon energy and smaller hydroxyl content.

Experiments and measurements

The molar composition of the studied glass is as follows: a series of (100-x) (AlF_3-MgF_2-CaF_2-SrF_2--YF_3-TeO_2)-xBaX_2 (X = F, Cl) glasses were prepared by the conventional melting method and the samples were named F15, F10C5, F5C10, C15 with doping amounts of 1%mol HoF_3 and 2%mol YbF_3, respectively The molar percentages of different rare-earth ions for the preparation of AYCl glass contained: C15 - yHoF_3 - 2YbF_3 (y=1.5,2,2.5,3,3.5,4) which named AYCl1-AYCl6. The samples were prepared with 99.99% purity AlF_3, CaF_2, BaF_2, SrF_2, MgF_2, $BaCl_2$, YF_3, YbF_3, HoF_3 powders. The mixed 20g batch of each sample was placed in an alumina crucible and melted in a furnace at 900°C for 20 minutes. During melting crucible was covered with an alumina sheet in order to prevent evaporation loss of the fluoride components. The melt was poured onto a preheated stainless steel mold and annealed in a muffle furnace according to the glass transition temperature. Fully annealed samples were made and polished to 10mm×10mm×2mm for optical property measurements.

The density was measured by distilled water and Archimedes' principle, refractive index of the

sample using prismatic least deviation method. The thermal stability of the chloride-modified fluorotellurite glasses were determined by using NetzschSTA449/C differential scanning calorimeter (DSC) at a temperature rise rate of 10 K/min. The absorption spectra in the range of 400 ~ 2500 nm were recorded with a UV/Vis/NIR spectrophotometer with a resolution of 1 nm. Raman spectra were measured with a Renishaw Via Raman microscope in the spectral range of 400 ~ 1000 cm^{-1} using a 532 nm laser excitation with a resolution of 1 cm^{-1}. Infrared transmittance was measured with a Perkin-Elmer 1600 series infrared spectrometer. The decay curves of Ho^{3+}:$^5I_6$ and $^5I_7$ energy levels at 2μm and 2.85μm were recorded with a digital oscilloscope under 980 nm LD excitation at a maximum power of 2W with a resolution of 1 nm. The mid-infrared luminescence spectra (1800 - 2200 nm) and (2600 - 3200 nm) injected by light pulses were measured by using a monochromator with a liquid nitrogen-cooled FLS980 Mid-infrared fluorescence spectrometer with a 980 nm LD pumped beam. All measurements were performed at room temperature. Other conditions were kept as consistent as possible.

Thermal stability characteristics

Fig. 1(a) shows the DSC curve of the chloride-modified fluorotellurite glass at 10 K/min temperature rise. The analysis of the DSC curve leads to characteristic temperature parameters such as glass transition T_g, crystallization onset T_x. The T_x is generally considered as the upper temperature limit for glass heat treatment process to avoid devitrification. The thermal stability ($\Delta T=T_x-T_g$) is usually used as a rough criterion parameter to judge the glass fiberisation ability [26]. Therefore, as the value of ΔT is larger, it indicates a wider working temperature range for preparing optical fibers. In order to satisfy the resistance to crystallization of glass preforms in the fiber drawing process, the ΔT should be larger than 100°C, however it strongly depends on the drawing parameters. From the analysis in Fig. 1(b), the characteristic glass temperatures of T_g and T_x decrease with the increase of the introduced Cl content. Similar with other reported results [25], the decrease of T_x was more moderate. The increasing of the thermal stability parameter occurred as a result of faster decrease of T_g value with the chloride ions concentration in the fluorotellurite glass. Hence it is inferred that the thermal stability of the chloride-modified fluorotellurite glass was improved. It is worth to note that showed in Table 1, the ΔT of the prepared C15 glass is 102°C, which is larger than that of the ZBLAN glass and fluorophosphate glass. Therefore, it is judged that fluorotellurite glass under chloride modification exhibits promising thermal stability and has potential applications in the field of mid-infrared lasers.

Table 1 Characteristic temperature of non-rare earth ion doped glasses.

	T_g	T_x	ΔT	Reference
F15	451	540	89	This work
F10C5	441	537	96	This work
F5C10	428	527	99	This work
C15	423	525	102	This work
fluorophosphate glass	332	408	76	[18]
ZBLAN	438	520	82	[19]

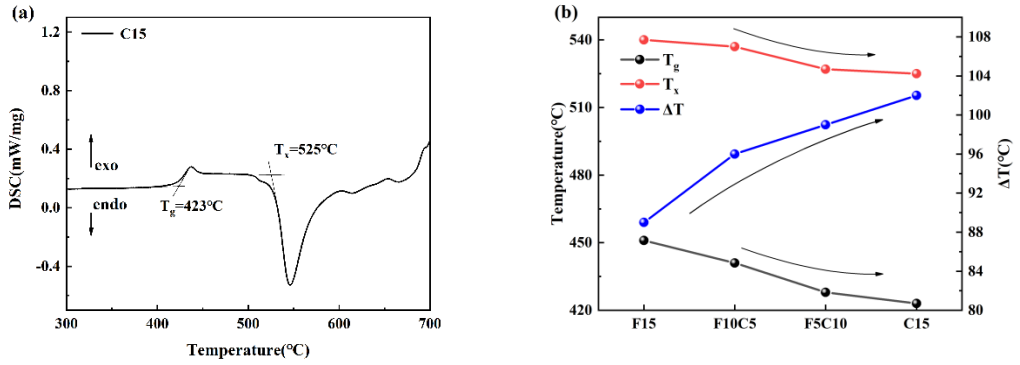

Figure 1 (a) Characteristic temperature of C15 glass. (b) Trend of characteristic temperature of chloride-modified fluorotellurite glasses.

Infrared transmission spectra and XRD spectrum

The infrared transmission spectra of chloride-modified fluorotellurite glasses in the range of 400-4000 cm^{-1} are illustrated in Fig. 2(a). The maximum infrared transmittance of fluorotellurite glass reaches 91%, leaving 10% loss due to Fresnel reflection absorption and dispersion of the glass [27]. The infrared transmittance is reduced due to the influence of absorption peak of CO_2 group near 3000cm^{-1} and absorption of OH^- group around 3500cm^{-1}. It is known that OH^- groups participate in energy transfer, which leads to luminescence quenching of Er and Ho ions at 3 μm[28]. Therefore, the introduction of chlorides reduces the content of OH^- and strengthens the mid-infrared luminescence. The hydroxyl content can be calculated by the infrared transmission spectra through the following equation [1]:

$$\alpha[OH^-] = \frac{\ln(T_0/T)}{d} \quad (1)$$

where d is sample thickness, T_0 is baseline transmittance and T is transmittance at 2.5μm. As shown in Fig. 2(b), the infrared transmittance gradually increases while the OH^- content decreases through the addition of $BaCl_2$. Table 2 shows the hydroxyl content of fluorotellurite glass modified by chloride and the hydroxyl content of C15 is calculated as the minimum value of 0.782 cm^{-1}. Therefore, we believe that the introduction of Cl^- causes the HF and HCl formation in the fluorotellurite glass to volatilize continuously leading to the OH^- group being removed constantly. It is also worth to note that with the increase of Cl^- content, the infrared cut-off wavelength of glass reaches 7.6μm, which is longer than fluorophosphate glasses (4.5μm) [29] and germanate glasses(6.5μm) [30]. Therefore, the chloride-modified fluorotellurite glass with low hydroxyl content and high transmittance is a promising mid-infrared luminescent material.

Table2 The hydroxyl content of fluorotellurite glass modified by chloride

	F15	F10C5	F5C10	C15
Hydroxyl Content(cm^{-1})	1.352	1.336	1.138	0.788

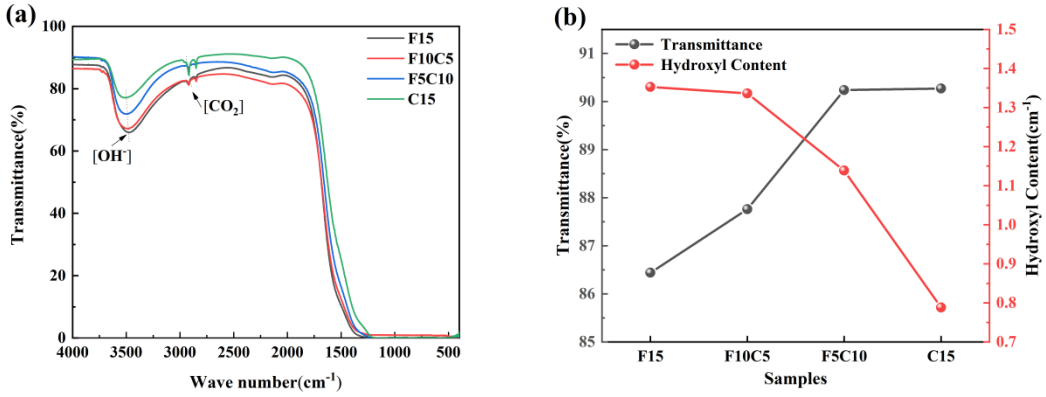

Figure 2 (a) Infrared transmittance spectra of chloride-modified fluorotellurite glass in the range of 400-4000cm^{-1}. (b) Infrared transmittance (@2.5μm) and hydroxyl content of samples with different chloride concentrations.

Fig. 3 shows the XRD spectra of AYCl glass. It can be seen that all the glasses exhibit similar spectrum and there is no sharp crystallization peaks but broad humps between 20° and 60°, which confirms the glass is in an amorphous nature.

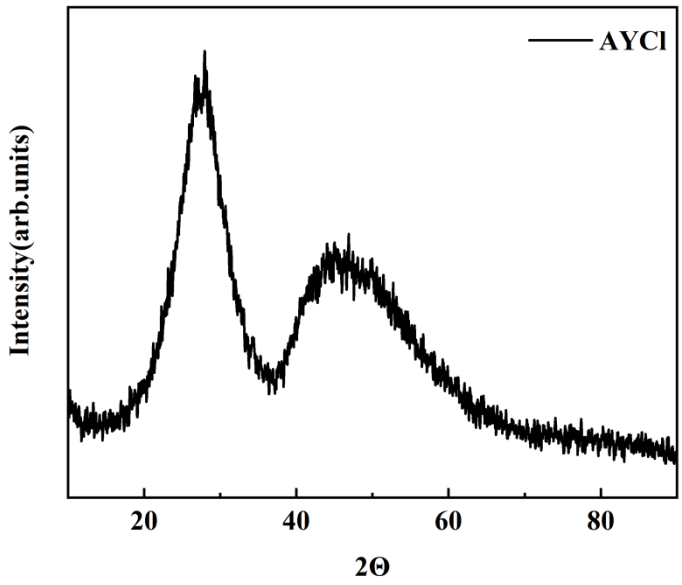

Figure 3 XRD of chloride-modified fluorotellurite glass

Raman spectra

In Fig. 4, the inset shows the Raman spectra of all samples with peaks near 415 cm^{-1}, corresponding to the stretching vibrations of the Te-O-Te bond formed by the [TeO_4] triangular double cone, the [TeO_3] triangular cone and the [TeO_{3+1}] polyhedron vertex. The vibrational peak at 568 cm^{-1} is close to the position of the Raman peak of the Al-F bond in the [AlF_6] regular octahedron reported by Gan [31]. Maaoui [32] reported that after the introduction of BaF_2 into tellurite glasses, F^- replaced some of the bridging oxygen in the [TeO_4] unit, turning the [TeO_4] unit

into a $[TeO, F]_4$ structural unit connected by bridging oxygen or bridging fluorine. Nabazal [33] found that F^- took the place of O^{2-} in part of the glass network structure after the introduction of fluoride into tellurite glasses. It is judged that the less O^{2-} in the fluorotellurite glass network structure, the more $[TeO_3]$ units will be present. In addition, the presence of $[TeO, F]_4$ structural units in the fluorotellurite glass structure will cause the Raman peak position of $[TeO_3]$ units moving to higher energy levels. Moreover, the Raman vibrational peak at 813 cm^{-1} corresponds to the $[TeO_3]$, $[TeO_{3+1}]$ and $[TeO, F]_4$ structural units. The Raman spectra of undoped rare earth chloride-modified fluorotellurite glasses are shown in Fig. 4. The peaks at 813cm^{-1} decrease with the increase of chloride ions content, which indicates that introduction chloride ions will reduce the number of non-bridge fluorides. This peak corresponds to the maximum phonon energy of chloride-modified fluorotellurite glass which is known as an important factor responsible for decreasing of non-radiative transitions, and facilitates the acquisition of efficient mid-infrared laser emission. However, the changes of different phonon energy of the chloride modification fluorotellurite glass are slight. We have judged the change of emission strength of modified fluorotellurite glass from phonon density. As reported in the literature[33], in the case of weak coupling of rare-earth luminescent centers, the multiphonon emission rate(MPR) W_{MP} follows the exponential gap law given by the following equation:

$$W_{MP}(0) = \mathrm{C}\left[\frac{exp(\hbar\omega_P/KT)}{exp(\hbar\omega_P/KT)-1}\right]^P e^{-\alpha\Delta\mathrm{E}} \quad (2)$$

where $\mathrm{P} = \Delta\mathrm{E}/\hbar\omega_P$ is the phonon order, E is the energy level difference, $\hbar\omega_P$ is the maximum phonon energy of the glass matrix, K is the Boltzmann constant, $\alpha = \ln(\varepsilon)/\hbar\omega_P$, and C depends on the matrix. In general, the maximum phonon energy of the glass matrix determines the multiple phonon decay of rare earth ions in the glass, as expressed in the equation. However, for samples with similar phonon energies, it is shown that the P values of the chloride-modified samples are also closer to each other. Therefore, the constant C may be an important factor in determining the W_{MP}. According to the Debye approximation:

$$\mathrm{C} \propto \rho\omega^{5/3} \quad (3)$$

where $\rho\omega$ is the phonon density of the glass matrix. Thus, a lower phonon density leads to a smaller C, implying a weaker MPR and stronger luminescence. The Raman peak intensity of the chloride-modified glasses decrease significantly with the increase of Cl^-. From the small changes in the emission intensity and the maximum phonon energy of these modified glasses, it is inferred that the difference in emission intensity is mainly influenced by the phonon density. In this study, the fluorotellurite glass has low phonon energy, and the phonon density is further reduced by the chloride modification. It is expected the mid-infrared luminescence can be enhanced.

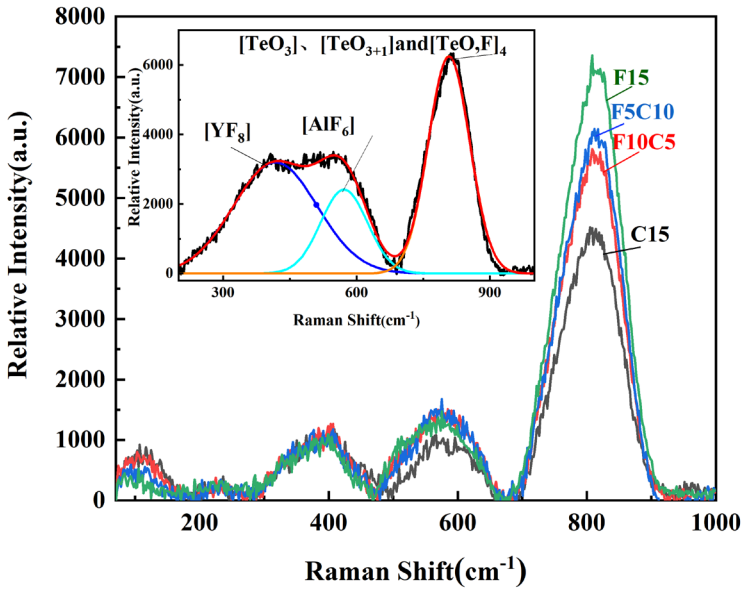

Figure 4 Raman spectra of chloride-modified fluorotellurite glasses. The inset is Raman split peak diagram.

Absorption spectra and energy transfer mechanisms

The measured absorption spectra of glasses with different concentrations of Ho^{3+}/Yb^{3+} co-doped and Ho^{3+} doped chloride-modified fluorotellurite glasses in the range of 400-2500 nm are illustrated in Fig. 5. It mainly consists of eight absorption bands from Ho^{3+} ground state $^5I_8$ to $^5I_7$, $^5I_6$, $^5F_5$, $^5F_4$+$^5S_2$, $^5F_3$, $^5G_6$, $^5G_5$ and Yb^{3+} ground state $^5F_{7/2}$ to excited state $^5F_{5/2}$, respectively. There is no transition above the $^5G_5$ energy level due to the intrinsic state absorption of the substrate. The absorption intensity increases with increasing Ho^{3+} concentration, and no change in the waveform or shift in the peak position is observed for the Ho^{3+}/Yb^{3+} co-doped fluorotellurite glass, which is the same result as the other Ho^{3+}/Yb^{3+} co-doped mechanism glasses [34, 35]. The results indicate that Ho^{3+} is well incorporated into the chloride-modified fluorotellurite glass network and no clustering of the local coordination field occurs [2]. Ho^{3+} doped AYCl glass cannot match the emission wavelengths of commercial lasers (808 nm and 980 nm) because of the lack of suitable absorption bands, but strong absorption near 980nm can be achieved by energy transfer form Yb^{3+}. The comparison between AYCl glass and AYCl1-6 glasses clearly seen a large absorption band of Yb^{3+}: $^2F_{5/2}$, which enables efficient laser diode pumping at the 980 nm and transfer energy to Ho^{3+} to achieve the mid-infrared luminescence at 2μm and 2.85μm.

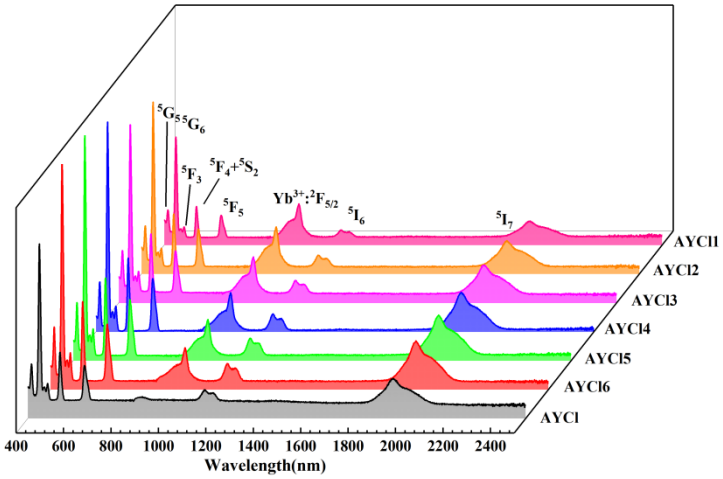

Figure 5 Absorption spectra of Ho^{3+} single-doped and Ho^{3+}/Yb^{3+} co-doped chloride-modified fluorotellurite glasses.

The Judd-Ofelt theory, is widely used to predict the spectral properties of the f-f transition of trivalent rare earth ions, was developed independently by Judd and Ofelt simultaneously in 1962 [36]. According to this theory, some important spectral parameters such as J-O intensity parameters, radiative transition probabilities, fluorescence branching ratios and lifetimes can be calculated from absorption spectra and refractive index. The detailed calculation steps have been mentioned in other literature [37]. In this article, only the calculation results are discussed. Table 3 shows the J-O parameters of Ho^{3+} in various glasses. According to previous studies, Ω_2 represents the number of covalent bonds between Ho^{3+} and the ligand anion. Larger Ω_2 indicates the stronger covalency and the lower the symmetry of Ho^{3+} [38]. In the analyzed glasses the $BaCl_2$ was initially introduced in the expense of BaF_2. In addition, the high content of BaF_2 is conducive to the existence of fluorine ions around Ho^{3+}, which reduces the covalence of the rare earth ion position and leads to the lower Ω_2 value. As the $BaCl_2$ concentration was further increased, the strength of the covalent bonds changed again, implying that the Ho-F ionic bonds were gradually replaced by those of Ho-Cl. Since the electronegativity of F (3.98) was bigger than that of Cl (3.16), the covalency of Ho-Cl was stronger than that of Ho-F. This phenomenon indicates that the stability of the microstructure disorder and glass network structure after the introduction of Cl^- was strengthened, while the asymmetry around Ho^{3+} was decreasing after the gradual introduction of Cl^-. In contrary the Ω_6 parameter is less associated with the local environment of Ho^{3+} ion, but more dependent on the overlapping integrals of the 4f and 5d orbitals. The value of Ω_6 parameter of the modified fluorotellurite glasses is higher than that of fluorophosphate glass, tellurite glass and fluoride glasses systems (Table 3). Thus, the prepared samples have lower covalency and higher 4f and 5d orbital overlap integrals.

Table 3 J-O parameters ($\Omega_{2,4,6}$) of Ho^{3+} in various glasses.

Sample glass	Ω_2	Ω_4	Ω_6	Reference
F15	3.6	1.18	1.48	This work
F10C5	3.25	1.2	1.58	This work
F5C10	3.83	1.76	1.72	This work
C15	3.54	1.94	1.59	This work

Fluorophosphate	2.54	3.19	1.27	[39]
Fluoride	1.86	1.90	1.32	[40]
Tellurite	6.79	3.92	1.51	[41]

The radiative transition probabilities, fluorescence branching ratios and decay lifetimes of Ho^{3+}-doped chloride-modified fluorotellurite glasses at different energy levels are shown in Table 4. It is worth noting that the A_{rad} of AYCl3 for Ho^{3+}:$^5I_7 \rightarrow {}^5I_8$ reaches 118.05 s^{-1}, which is higher than both fluorophosphate glass (70.98s^{-1}) [42] and tellurite glass (104s^{-1}) [43]. It is well known that larger radiative transition probabilities provide better opportunities for mid-infrared luminescence. The effective luminescence of Ho^{3+}/Yb^{3+} co-doped chloride-modified fluorotellurite glasses of 2μm and 2.85μm were obtained.

Table 4 Radiative transition probabilities (A_{rad}), branching ratios (β) and radiative lifetimes (τ_{rad}) of Ho^{3+} in AYCl3 glass.

Transition	Energy gap(cm^{-1})	A_{rad}(s^{-1})	β (%)	τ_{rad} (ms)
$^5I_7$-$^5I_8$	5128	118.05	100%	8.47
$^5I_6$-$^5I_8$	8681	210.35	84.62%	4.02
$^5I_6$-$^5I_7$	3552	38.24	15.38%	
$^5I_5$-$^5I_8$	11236	75.42	38.61%	5.12
$^5I_5$-$^5I_7$	6108	104.79	53.65%	
$^5I_5$-$^5I_6$	2555	15.11	7.74%	

Fluorescence spectra and fluorescence lifetimes

Fig. 6(a) and (b) depict the fluorescence spectra of 1mol Ho^{3+}/ 2mol Yb^{3+} co-doped fluorotellurite glasses under 980 nm laser pumping. The mid-infrared band luminescence at 2μm and 2.85μm correspond to the energy levels transition of Ho^{3+}: $^5I_7 \rightarrow {}^5I_8$, $^5I_6 \rightarrow {}^5I_7$, respectively. Interestingly, when the content of $BaCl_2$ increases, BaF_2 in glass components is gradually replaced, and Cl^- content in glass components increases, it can be found that the emission intensity of mid-infrared luminescence in both bands increases significantly. When $BaCl_2$ completely superseded BaF_2, the emission intensity reached its maximum value, and the thermal stability of the glass was improved while maintaining the high infrared transmittance of the glass. It is noteworthy that the fluorescence spectrum of 2μm consists of several Stark emission bands in the shape of non-Gaussian peaks. A Gaussian deconvolution method was used to verify the peak portion of the spectrum of 2μm, and the results are shown in Fig. 6(c). It can be observed that the wavelengths distributed by two Gaussians are 1944 nm and 2032 nm, respectively. According to the spectra, it can be developed a three-energy-level equivalent model as shown in the inset of Fig. 6(c), where the $^5I_7$ energy level is represented by the upper Stark energy level c and the lower energy level b. The energy levels transition such as b → a, c → a, corresponding to peak 1 and peak 2, respectively (Fig. 6(c)). Moreover, the shape of the Gaussian peak is somewhat different compared to the other reported results, which could indicate a close relationship between the Stark splitting and the composition of the glass matrix [44].

To elucidate the mid-infrared luminescence more accurately, the energy level transition and energy transfer between Yb^{3+} ions and Ho^{3+} ions were analyzed as shown in Fig. 6(d). When the sample is irradiated by the 980 nm laser, the ground state energy level Yb^{3+}: $^5F_{7/2}$ is pumped to the excited energy level Yb^{3+}:$^5F_{5/2}$. Then part of the energy can be transferred to a neighboring Ho^{3+} by

transferring energy under the assistance of host phonons (ET: Yb^{3+}:$^2F_{5/2}$+Ho^{3+}:$^5I_8$→Yb^{3+}:$^2F_{7/2}$+Ho^{3+}:$^5I_6$). A part of the ions are transferred to the higher energy level $^5F_4$+$^5S_2$ via excited-state absorption (ESA:$^5I_6$+a photon→$^5F_4$,$^5S_2$). The ions on the $^5F_4$ and $^5S_2$ energy levels will decay non-radiatively (NR) to the next level $^5I_5$ as well as further decay rapidly to the $^5I_6$ energy level. Another part ions in Ho^{3+}: $^5I_6$ energy level relax to lower energy level Ho:$^5I_7$ by radiative process obtains 2.85μm fluorescence. Simultaneously, non-radiative emission takes place from the $^5I_6$ level to the low $^5I_7$ level. Besides, most of the Ho^{3+} ions in the $^5I_7$ energy level return to the $^5I_8$ ground energy level with a strong mid-infrared emission at 2.0 μm. It is worth to note that up-conversion mechanisms have not been analysed.

In addition, quantum efficiency is an important characteristic parameter for fluorescence emission. Spontaneous radiation life and measured fluorescence life are used to calculate the efficiency of quantum efficiency, which can be calculated according to the formula:

$$\eta = \frac{\tau_{mea}}{\tau_{rad}} \times 100\% \quad (4)$$

where τ_{mea} is the measured fluorescence emission life and τ_{rad} is spontaneous radiation transition life calculated by J-O parameters. Fig. 6 (e) shows the fluorescence lifetime of Ho^{3+}: $^5I_7$ →$^5I_8$. With the increase of Cl content, the fluorescence lifetime increases. Moreover, the inset shows the obtained quantum efficiency of Ho^{3+}: $^5I_7$→$^5I_8$ increased from 11.6% of F15 to 14.9% of Cl15. The fluorescence lifetime decay curve of Ho^{3+}: $^5I_6$→$^5I_7$ is shown in Fig. 6 (f), in which the trend of changes is the same as Ho^{3+}: $^5I_7$→$^5I_8$. The inset shows that the obtained quantum efficiency of F15 increases from 20.48% to 30.99% of Cl15. It can be seen that the introduction of Cl makes the quantum efficiency continuously improve. Therefore, the luminescence property of fluorotellurite glass is further improved after chloride modification.

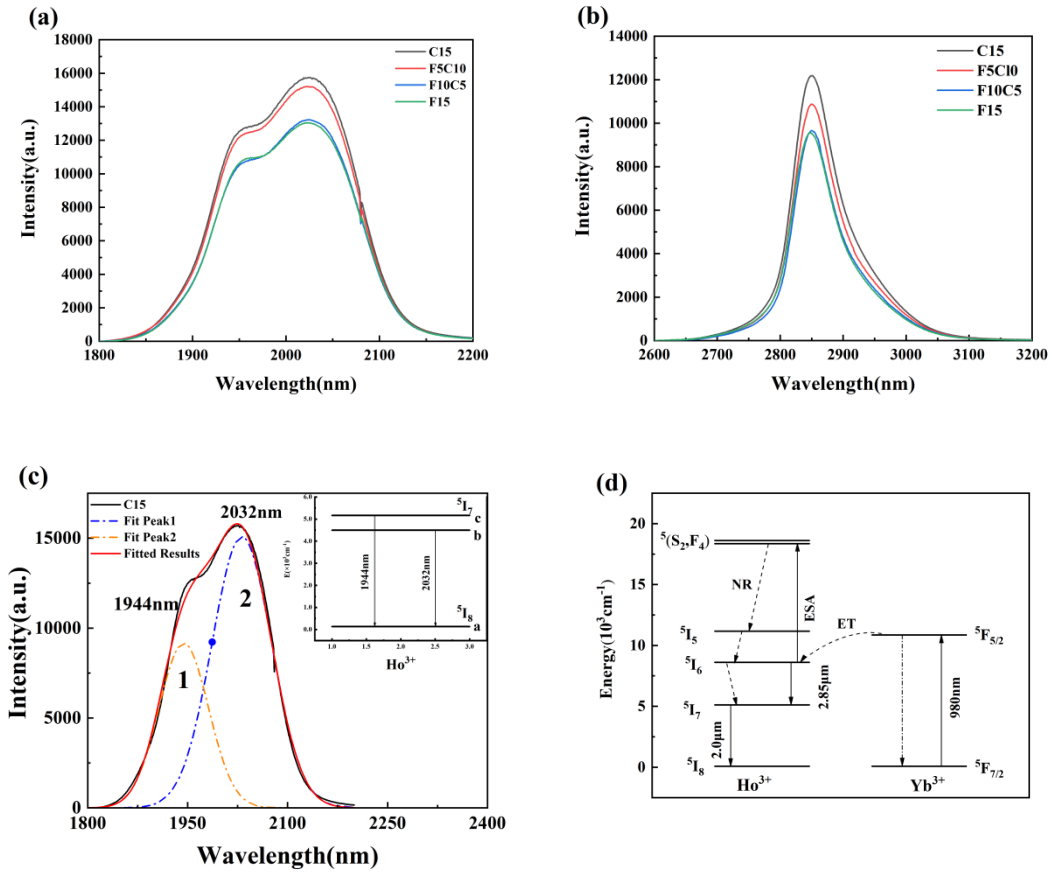

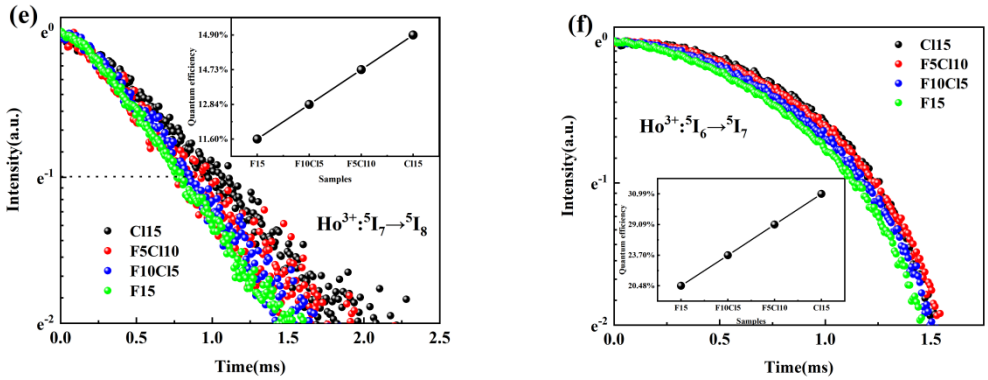

Figure 6 (a) Fluorescence spectra between 1800nm-2200nm. (b) Fluorescence spectra between 2600nm-3200nm. (c) 2μm energy level equivalent model, and the inset is Gaussian convolution wavelength distribution. (d) Energy level diagram and energy transfer mechanism between Ho^{3+} and Yb^{3+} ions in chloride-modified fluorotellurite glass. (e) Ho^{3+}:$^5I_7$⟶$^5I_8$ fluorescence lifetime and the inset is quantum efficiency of different samples with different chloride content in 2 μm. (f) Ho^{3+}:$^5I_6$⟶$^5I_7$ fluorescence lifetime and the inset is quantum efficiency of different samples with different chloride content in 2.85 μm.

Fig. 7 (a) and (b) show the mid-infrared luminescence intensity for different HoF_3 concentration, when YbF_3 is 2 mol%. The maximum luminescence intensity in both bands of 2μm and 2.85μm occur in the AYCl3 sample. Then, due to the concentration quenching effect, the fluorescence luminescence intensity starts to weaken with the further gradual increase of Ho^{3+}, and thus the optimal concentration of HoF_3 is judged to be 2.5mol%. Meanwhile, calculating the full width of half maximum (FWHM) of the emission spectra shown in Fig. 7(c), the strongest peak corresponds to the wavelength of the luminescence center, and make a horizontal line parallel to the X axis at half of the peak. The intersection points are located on both sides of the peak. The distance between the two intersection points is the maximum half-height width. FWHM is usually used to judge the performance of light amplification. The FWHM of 2μm is 166.32 nm, which is larger than that of tellurite germanate glass (146nm) [45]. As is shown in Fig. 7 (d), the FWHM at 2.85μm is 85.76 nm, which is much larger than that of fluoroaluminate glass (59nm) [34] and fluorotellurite glass (83nm) [46]. Obtaining a wide FWHM offers the possibility to develop fiber optical parametric amplifiers [47].

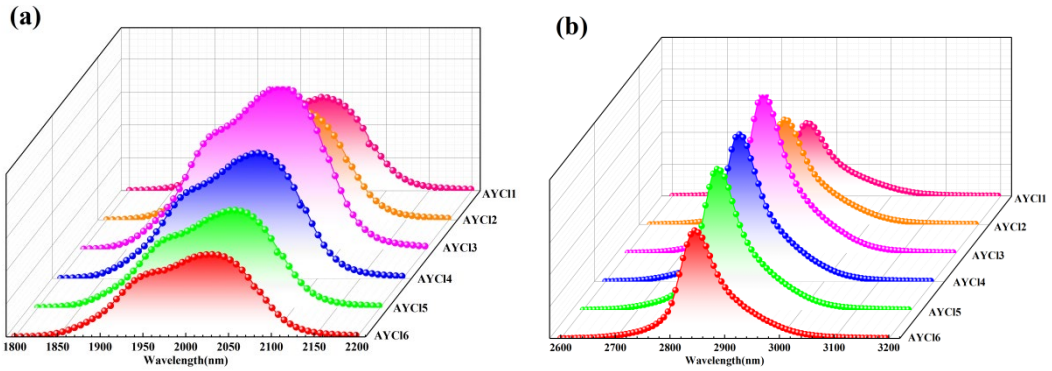

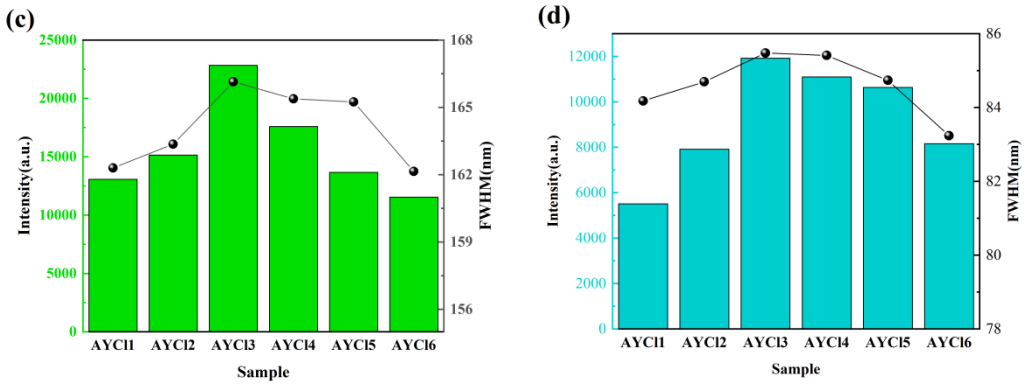

Figure 7 (a) Fluorescence spectra of Ho^{3+}/Yb^{3+} co-doped C15 glasses between 1800nm-2200nm. (b) Fluorescence spectra of Ho^{3+}/Yb^{3+} co-doped C15 glasses between 2600nm-3200nm. (c) The relationship between FWHM of 2μm fluorescence and HoF_3 content. (d) The relationship between FWHM of 2.85μm fluorescence and HoF_3 content.

To analyze the Ho^{3+}/Yb^{3+} co-doped luminescence properties, the fluorescence decay curves corresponding to the $^5I_7$ energy level and $^5I_6$ energy level were measured under 980 nm laser excitation of the chloride-modified fluorotellurite glasses as shown in Fig. 8. It is found that the fluorescence lifetime at 2μm and 2.85μm of the AYCl3 sample can reach 4.36ms and 0.52ms, respectively. The obtained fluorescence lifetime times are much larger than those of fluoride glass (2.997ms) [48] at $^5I_7$ level and larger than tellurite glass (0.434ms) [35]. In addition, we can observe the relationship between fluorescence lifetime and Ho^{3+} ion dopant concentration. When HoF_3 reaches 2.5mol%, the fluorescence lifetime begins to decrease with the increase of Ho^{3+} concentration. The reason can be attributed to the fact that increasing the doping concentration will bring dipole-dipole interactions between Ho – Ho ions, which provides more opportunities for the energy transfer process, resulting in more non-radiative transitions at the $^5I_6$ and $^5I_7$ levels, thereby shortening the emission fluorescence lifetime. Additionally back transfer to Yb ions can not be excluded.

The obtained quantum efficiencies of Ho^{3+} : $^5I_7 \rightarrow {}^5I_8$ and Ho^{3+} : $^5I_6 \rightarrow {}^5I_7$ at AYCl3 are 51.47% and 84.14% respectively, which are larger than that of Ho^{3+} : $^5I_7 \rightarrow {}^5I_8$ in tellurite glass (42.6%) [43] and Ho^{3+} : $^5I_6 \rightarrow {}^5I_7$ in YSGG(32.7%) [49]. The chloride-modified fluorotellurite glass with higher quantum efficiency is a potential material for 2-3 μm luminescence.

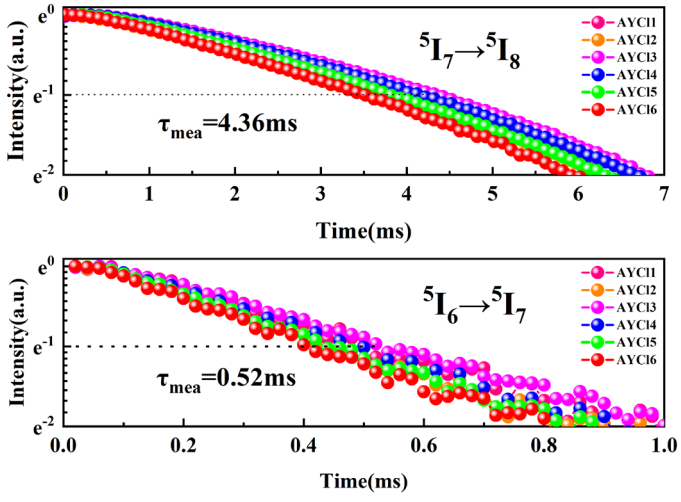

Figure 8 Fluorescence decay curves of the Ho^{3+}: $^5I_7 \rightarrow {}^5I_8$ level and $^5I_6 \rightarrow {}^5I_7$ transitions in AYCl3 glass.

Absorption cross-section, emission cross-section and gain coefficient

To explore more deeply the potential applications of mid-infrared luminescent materials, we calculated the emission cross-section, absorption cross-section, and gain coefficient of the AYCl3 glass. The emission cross-section was calculated from the emission spectra according to the Füchtbauer– Ladenburg (FL) formula [50]:

$$\delta_{em}(\lambda) = \frac{\lambda^4 A_{rad}}{8\pi c n^2} \times \frac{\lambda I(\lambda)}{\int I(\lambda) d\lambda} \tag{5}$$

where A_{rad} is the spontaneous transition probability corresponding to Ho^{3+}: $^5I_7 \rightarrow {}^5I_8$, $^5I_6 \rightarrow {}^5I_7$ transitions, λ is the wavelength, n and c represent the refractive index of the glass and the speed of light, respectively. λI(λ) and the integral λI(λ) are the fluorescence spectral intensity and the light intensity integral. 2μm and 2.85μm emission cross-sections of the AYCl3 sample are 11.82×10^{-21} cm^2 and 8.95×10^{-21} cm^2, respectively. The higher emission cross-section is more favorable to obtain high gain laser output. In addition, the absorption cross-section was obtained from the calculated emission cross-section using the McCumber (MC) formula [39]:

$$\delta_{(\lambda)} = \delta_{abs}(\lambda) \times \frac{Z_l}{Z_u} \times exp\left[\frac{hc}{kT} \times \left(\frac{1}{\lambda_{ZL}} - \frac{1}{\lambda}\right)\right] \tag{6}$$

where Z_l and Z_u represent the lower and upper energy level optical transition parameters, respectively. λ_{ZL} is the transition wavelength between the Stark lower energy level of the emitting polymorph and the Stark lower energy level of the receiving polymorph. T and k are constants representing the temperature and Boltzmann constant, respectively.

The larger absorption cross-section is beneficial to absorbing energy from pump light and improving pump efficiency. As shown in Fig. 9(a) and (c), it indicates that the absorption cross-section of the AYCl3 sample glass reaches 16.47×10^{-21} cm^2 and 7.8×10^{-21} cm^2 at 2μm and 2.85μm, respectively. Therefore, the chloride-modified fluorotellurite glass is a good favorable substrate material with good mid-infrared luminescence properties. Furthermore, the gain characteristic coefficient of the material can be calculated to judge its emission performance quantitatively. The gain coefficient G(λ) can be obtained by using the formula [3]:

$$G(\lambda) = N[\delta_{em}(\lambda) - (1 - P)\delta_{abs}(\lambda)] \tag{7}$$

where N is the rare-earth ion concentration of Ho^{3+} and P is the inverse order occupation of the corresponding Ho^{3+} ions.

Fig. 9(b) and (d) show the gain curves for AYCl3 samples at the $^5I_7$ and $^5I_6$ level, respectively. As the ion number reversal decreases, the gain peak keeps moving toward the long wavelength. This is a very common feature in three-energy laser systems [51]. It is obvious to find that the gain coefficient is positive at P>0.7 in the 2μm band and positive at P>0.5 in the 2.85μm band. This result indicates that the prepared chloride-modified fluorotellurite glass with good emission properties in the mid-infrared band is a promising material for high-gain mid-infrared luminescence.

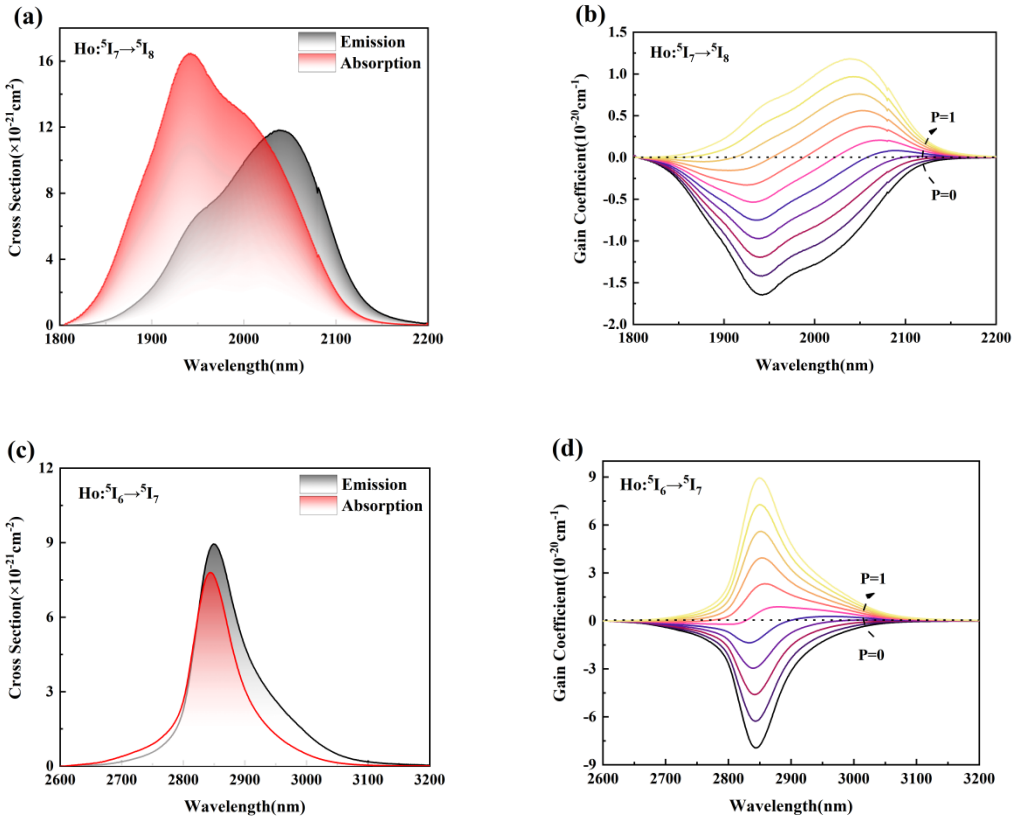

Figure 9 (a) AYCl3 glass Ho^{3+}: $^5I_7 \rightarrow ^5I_8$ energy level transmission absorption and emission cross-section. (b) Gain coefficient corresponding to $^5I_7 \rightarrow ^5I_8$ transition of Ho^{3+} in AYCl3 glass. (c) Absorption and emission cross-section of Ho^{3+}: $^5I_6 \rightarrow ^5I_7$ energy level transition of AYCl3 glass. (d) Gain coefficient corresponding to $^5I_6 \rightarrow ^5I_7$ transition of Ho^{3+} in AYCl3 glass.

Conclusion

In summary, Ho^{3+}/Yb^{3+} co-doped chloride-modified fluorotellurite glasses are prepared. The substitution of BaF_2 by $BaCl_2$ showed a beneficial influence on the infrared transmittance thermal stability and characterized by Raman spectroscopy. The J-O intensity parameters and radiation properties of Ho^{3+} ions are calculated based on the J-O theory. A multi-energy level equivalent model is proposed to describe the 2μm and 2.85μm fluorescence. The experimental results show that the introduction of chloride in fluorotellurite glass helps to remove OH^- effectively and improves the transmittance of fluorotellurite glass. Meanwhile, the chloride-modified fluorotellurite glass has the advantage of low phonon energy density. Due to the reduced phonon density of the glass matrix, the lifetime of Ho^{3+} at the high energy level is prolonged, which leads to an increase in the radiation transition probability. A broadband 2μm emission with FWHM of 166.32 nm is obtained under the pump of 980 nm LD. The calculated emission cross-sections of the prepared AYCl3 glass at 2μm and 2.85μm reached 16.47 × 10^{-21} cm^2 and 7.8 × 10^{-21} cm^2. The quantum efficiencies of Ho^{3+}: $^5I_7 \rightarrow ^5I_8$ and $^5I_6 \rightarrow ^5I_7$ reach 51.47% and 84.14%, respectively. The prepared chloride in fluorotellurite glass reveals excellent performance in mid-infrared luminescence. Therefore, this glass has potential applications in mid-infrared fiber amplifiers and laser devices.

Declaration of Competing Interest

The authors declare that they have no known competing financial interests or personal relationships that could have appeared to influence the work reported in this paper.

Acknowledgement

The authors are thankful to National Key Research and Development Project of China(2018YFE0207700), the Zhejiang Provincial Natural Science Foundation of China (LZ21F050002), the National Natural Science Foundation of China (61775205, 51872270), and Science and technology innovation leading talent project of special support plan for high-level talents in Zhejiang Province (2021R52032).

Reference

[1]R. Xu, Y. Tian, L. Hu and J. Zhang, Enhanced emission of 2.7 μm pumped by laser diode from Er^{3+}/Pr^{3+}-codoped germanate glasses, Opt Lett, 36(2011) 1173-1175, 10.1364/OL.36.001173

[2]Y. Tian, R. Xu, L. Hu and J. Zhang, Spectroscopic properties and energy transfer process in Er^{3+} doped ZrF_4-based fluoride glass for 2.7μm laser materials, Optical Materials, 34(2011) 308-312, 10.1016/j.optmat.2011.09.004

[3]J. Xia, Y. Tian, B. Li, L. Zheng, X. Jing, J. Zhang and S. Xu, Enhanced 2.0 μm emission in Ho^{3+}/Yb^{3+} co-doped silica-germanate glass, Infrared Physics & Technology, 81(2017) 17-20, 10.1016/j.infrared.2016.10.013

[4]A. Zhang, W. Shi, H. Guo and C. Yan, Mid-infrared flat-topped broadband chiral helix metamaterials based on indium tin oxide and their chiral properties, Chinese Optics Letters, 19(2021) 111601, 10.3788/COL202119.111601

[5]J. Zhu, H. Zhu, M. Liu, Y. Wang, H. Xu, N. Ali, H. Deng, Z. Tan, J. Cao and N. Dai, Ultrabroadband and multiband infrared/terahertz photodetectors with high sensitivity, Photonics Research, 9(2021) 2167-2175, 10.1364/PRJ.430960

[6]J. Liu, F. Artizzu, M. Zeng, L. Pilia, P. Geiregat and R. R. Van Deun, Dye-sensitized Er^{3+}-doped CaF_2 nanoparticles for enhanced near-infrared emission at 1.5 μm, Photonics Research, 9(2021) 2037-2045, 10.1364/PRJ.433192

[7]Y. Mizuno, A.Theodosiou, K. Kalli, S. Liehr, H. Lee and K.Nakamura, Distributed polymer optical fiber sensors: A review and outlook, Photonics Research, 9(2021) 1719-1733, 10.1364/PRJ.433334

[8]O. Henderson-Sapir, J. Munch and D. J. Ottaway, Mid-infrared fiber lasers at and beyond 3.5 μm using dual-wavelength pumping, Opt Lett, 39(2014) 493-496, 10.1364/OL.39.000493

[9]D. D. H. Jianfeng Li, Yong Liu, Stuart D. Jackson, Efficient 2.87 μm fiber laser passively switched using a semiconductor saturable absorber mirror, Opt Lett, 37(2012) 3747-3749, 10.1364/OL.37.003747

[10]D. W. H. T. Schweizer, B. N. Samson, and D. N. Payne, Spectroscopic data of the 1.8-, 2.9-, and 4.3-μm transitions in dysprosium-doped gallium lanthanum sulfide glass, Opt Lett, 21(1996) 1594-1596, 10.1364/OL.21.001594

[11]J. Li, D. D. Hudson and S. D. Jackson, High-power diode-pumped fiber laser operating at 3 μm, Opt Lett, 36(2011) 3642-3644, 10.1364/OL.36.003642

[12]K. Han, P. Zhang, S. Wang, Y. Guo, D. Zhou and F. Yu, Optical characterization of Tm^{3+} doped Bi_2O_3-GeO_2-Ga_2O_3 glasses in absence and presence of BaF_2, Sci Rep, 6(2016) 31207, 10.1038/srep31207

[13]E. Song, G. Zhu, H. Wang, H. Chen, Y. Qian, K. Aleksei and X. Zhu, Up conversion and excited state absorption analysis in the Tm:YAG disk laser multi-pass pumped by 1 μm laser, High Power Laser Science and Engineering, 9(2021) 10.1017/hpl.2020.55

[14]C. Petersen, M. Lotz, C. Markos, G. Woyessa, D. Furniss, R. Seddon, R. Taboryski and O. O. Bang, Thermo-mechanical dynamics of nanoimprinting anti-reflective structures onto small-core mid-IR chalcogenide fibers, Chinese Optics Letters, 19(2021) 030603, 10.3788/COL202119.030603
[15]D. Tan, Z. Wang, B. Xu and J. J. Qiu, Photonic circuits written by femtosecond laser in glass: improved fabrication and recent progress in photonic devices, Advanced Photonics, 3(2021) 024002, 10.1117/1.AP.3.2.024002
[16]Y. Zhao, L. Wang, W. Chen, P. Loiko, X. Mateos, X. Xu, Y. Liu, D. Shen, Z. Wang and X. J. P. R. Xu, Structured laser beams: toward 2-μm femtosecond laser vortices: publisher's note, Photonics Research, 9(2021) 1343-1343,
[17]G. Hou, C. Zhang, W. Fu, G. Li, J. Xia and Y. Ping, Broadband mid-infrared 2.0 μm and 4.1 μm emission in Ho^{3+}/Yb^{3+} co-doped tellurite-germanate glasses, Journal of Luminescence, 217(2020) 10.1016/j.jlumin.2019.116769
[18]Y. Guo, M. Li, L. Hu and J. Zhang, Effect of fluorine ions on 2.7 um emission in Er^{3+}/Nd^{3+}-codoped fluorotellurite glass, J Phys Chem A, 116(2012) 5571-5576, 10.1021/jp301582b
[19]H. Zhao, S. Jia, X. Wang, R. Wang, X. Lu, Y. Fan, M. Tokurakawa, G. Brambilla, S. Wang and P. Wang, Investigation of Dy^{3+}/Tm^{3+} co-doped ZrF_4-BaF_2-YF_3-AlF_3 fluoride glass for efficient 2.9 μm mid-infrared laser applications, Journal of Alloys and Compounds, 817(2020) 10.1016/j.jallcom.2019.152754
[20]K. Li, G. Wang, J. Zhang and L. Hu, Broadband ~2 μm emission in Tm^{3+}/Ho^{3+} co-doped TeO_2–WO_3–La_2O_3 glass, Solid State Communications, 150(2010) 1915-1918, 10.1016/j.ssc.2010.07.030
[21]R. Xu, Y. Tian, L. Hu and J. Zhang, 2 μm spectroscopic investigation of Tm^{3+}-doped tellurite glass fiber, Journal of Non-Crystalline Solids, 357(2011) 2489-2493, 10.1016/j.jnoncrysol.2010.11.059
[22]F. Qi, F. Huang, T. Wang, R. Ye, R. Lei, Y. Tian, J. Zhang, L. Zhang and S. Xu, Highly Er^{3+} doped fluorotellurite glass for 1.5 μm broadband amplification and 2.7 μm microchip laser applications, Journal of Luminescence, 202(2018) 132-135, 10.1016/j.jlumin.2018.05.049
[23]J. Liu, X. Huang, H. Pan, X. Zhang, X. Fang, W. Li, H. Zhang, A. Huang and Z. Xiao, Broadband near infrared emission of Er^{3+}/Yb^{3+} co-doped fluorotellurite glass, Journal of Alloys and Compounds, 866(2021) 10.1016/j.jallcom.2020.158568
[24]Y. S. Rammah, F. I. El-Agawany, N. Elkhoshkhany, F. Elmasry, M. Reben, I. Grelowska and E. Yousef, Physical, optical, thermal, and gamma-ray shielding features of fluorotellurite lithiumniobate glasses: TeO_2-$LiNbO_3$-BaO-BaF_2-La_2O_3, Journal of Materials Science: Materials in Electronics, 32(2021) 3743-3752, 10.1007/s10854-020-05119-3
[25]Y. Zou, Y. Wang, S. Han, Y. Du, D. Chen and Q. Yang, Effect of chloride on spectrum properties of Pr^{3+}/Ho^{3+} co-doped fluorozirconate glasses, Journal of Rare Earths, 38(2020) 139-142, 10.1016/j.jre.2019.07.007
[26]Q. Fangwei, H. Feifei, L. Ruoshan, T. Ying, Z. Long, Z. Junjie and X. Shiqing, Emission Properties of 1.8 and 2.3 μm in Tm^{3+} -Doped Fluoride Glass, Glass Physics and Chemistry, 43(2017) 340-346, 10.1134/S1087659617040058
[27]T. Wei, F. Chen, Y. Tian and S. Xu, Efficient 2.7μm emission and energy transfer mechanism in Er^{3+} doped Y_2O_3 and Nb_2O_5 modified germanate glasses, Journal of Quantitative Spectroscopy and Radiative Transfer, 133(2014) 663-669, 10.1016/j.jqsrt.2013.10.003
[28]T. Ragin, J. Zmojda, M. Kochanowicz, P. Miluski, P. Jelen, M. Sitarz and D. Dorosz, Enhanced mid-infrared 2.7 μm luminescence in low hydroxide bismuth-germanate glass and optical fiber co-doped with Er^{3+}/Yb^{3+} ions, Journal of Non-Crystalline Solids, 457(2017) 169-174, 10.1016/j.jnoncrysol.2016.12.001
[29]T. Ying, X. Rongrong, Z. Liyan, H. Lili and J. Zhang, Observation of 2.7 μm emission from diode-

pumped Er^{3+}/Pr^{3+}-codoped fluorophosphate glass, Opt Lett, 36(2011) 109-111,
[30]T. Wei, F. Chen, X. Jing, Y. Tian, F. Wang and S. Xu, Mid-infrared fluorescence of Y_2O_3 and Nb_2O_5 modified germanate glasses doped with Er^{3+} pumped by 808nm LD, Optical Materials, 36(2014) 1350-1356, 10.1016/j.optmat.2014.03.026
[31]H. Chen and F. Gan, Vibrational Spectra and Structure of AlF_3/YF_3 Fluoride Glasses, Journal of Non-Crystalline Solids, 112(1989) 272-276, 10.1016/0022-3093(89)90535-8
[32]A. Maaoui, M. Haouari, A. Bulou, B. Boulard and H. Ben Ouada, Effect of BaF_2 on the structural and spectroscopic properties of Er^{3+}/Yb^{3+} ions codoped fluoro-tellurite glasses, Journal of Luminescence, 196(2018) 1-10, 10.1016/j.jlumin.2017.12.001
[33]C. B. Layne and M. J. Weber, Multiphonon relaxation of rare-earth ions in beryllium-fluoride glass, Physical Review B, 16(1977) 3259-3261, 10.1103/PhysRevB.16.3259
[34]B. Zhou, T. Wei, M. Cai, Y. Tian, J. Zhou, D. Deng, S. Xu and J. Zhang, Analysis on energy transfer process of Ho^{3+} doped fluoroaluminate glass sensitized by Yb^{3+} for mid-infrared 2.85 μm emission, Journal of Quantitative Spectroscopy and Radiative Transfer, 149(2014) 41-50, 10.1016/j.jqsrt.2014.08.001
[35]G. Gupta, S. Balaji, K. Biswas and K. Annapurna, Enhanced luminescence at 2.88 and 2.04 μm from Ho^{3+}/Yb^{3+} codoped low phonon energy $TeO_2–TiO_2–La_2O_3$ glass, AIP Advances, 9(2019) 10.1063/1.5054190
[36]B. R. Judd, Optical Absorption Intensities of Rare-Earth Ions, Physical Review, 127(1962) 750-761, 10.1103/PhysRev.127.750
[37]B. Xu, B. Yang, Y. Zhang, H. Xia and J. Wang, Cooperative energy transfer in Tm^{3+} and Yb^{3+} co-doped phosphate glasses, Journal of Rare Earths, 31(2013) 164-168, 10.1016/s1002-0721(12)60252-x
[38]W. Zhang, J. Lin, Y. Jia, S. Zhang, J. Zhao, G. Sun, S. Ye, J. Ren and L. Rong, Enhanced 2-5 μm emission in Ho^{3+}/Yb^{3+} codoped halide modified transparent tellurite glasses, Spectrochim Acta A Mol Biomol Spectrosc, 134(2015) 388-398, 10.1016/j.saa.2014.06.010
[39]T. Ying, Z. Liyan, F. Suya, X. Rongrong, H. Lili and Z. Junjie, 2 μm Emission of Ho^{3+}-doped fluorophosphate glass sensitized by Yb^{3+}, Optical Materials, 32(2010) 1508-1513, 10.1016/j.optmat.2010.06.012
[40]Bo Peng and T. Izumitani, Optical properties, fluorescence mechanisms and energy transfer in Tm^{3+}, Ho^{3+} and Tm^{3+}-Ho^{3+} doped near-infrared laser glasses, sensitized by Yb^{3+}, Optical Materials, 4(1995) 797-810, 10.1016/0925-3467(95)00032-1
[41]Y. Zheng, B. Chen, J. Sun, L. Cheng, H. Zhong, X. Li, J. Zhang, Y. Tian, T. Yu and L. Huang, Composition-dependent optical transitions and 2.0μm emission properties of Ho^{3+} in $xGeO_2$-$(80–x)TeO_2$-$9.5ZnF_2$-$10NaF$-$0.5Ho_2O_3$ glasses, Journal of Rare Earths, 29(2011) 924-928, 10.1016/S1002-0721(10)60570-4
[42]M. Wang, L. Yi, G. Wang, L. Hu and J. Zhang, 2 μm emission performance in Ho^{3+} doped fluorophosphate glasses sensitized with Er^{3+} and Tm^{3+} under 800 nm excitation, Solid State Communications, 149(2009) 1216-1220, 10.1016/j.ssc.2009.04.021
[43]L. Tao, Y. H. Tsang, B. Zhou, B. Richards and A. Jha, Enhanced 2.0μm emission and energy transfer in $Yb^{3+}/Ho^{3+}/Ce^{3+}$ triply doped tellurite glass, Journal of Non-Crystalline Solids, 358(2012) 1644-1648, 10.1016/j.jnoncrysol.2012.04.028
[44]T. Wei, C. Tian, M. Cai, Y. Tian, X. Jing, J. Zhang and S. Xu, Broadband 2μm fluorescence and energy transfer evaluation in Ho^{3+}/Er^{3+} codoped germanosilicate glass, Journal of Quantitative Spectroscopy and Radiative Transfer, 161(2015) 95-104, 10.1016/j.jqsrt.2015.03.035

[45]R. Chen, Y. Tian, B. Li, F. Wang, X. Jing, J. Zhang and S. Xu, 2μm fluorescence of Ho^{3+}:$^5I_7 \rightarrow ^5I_8$ transition sensitized by Er^{3+} in tellurite germanate glasses, Optical Materials, 49(2015) 116-122, 10.1016/j.optmat.2015.09.003

[46]J. He, Z. Zhou, H. Zhan, A. Zhang and A. Lin, 2.85μm fluorescence of Ho-doped water-free fluorotellurite glasses, Journal of Luminescence, 145(2014) 507-511, 10.1016/j.jlumin.2013.08.020

[47]M. Cai, B. Zhou, Y. Tian, J. Zhou, S. Xu and J. Zhang, Broadband mid-infrared 2.8μm emission in Ho^{3+}/Yb^{3+}-codoped germanate glasses, Journal of Luminescence, 171(2016) 143-148, 10.1016/j.jlumin.2015.11.016

[48]J. Yuan, S. X. Shen, D. D. Chen, Q. Qian, M. Y. Peng and Q. Y. Zhang, Efficient 2.0 μm emission in Nd^{3+}/Ho^{3+} co-doped tungsten tellurite glasses for a diode-pump 2.0 μm laser, Journal of Applied Physics, 113(2013) 10.1063/1.4803043

[49]P. Zhang, B. Zhang, J. Hong, L. Zhang, J. He and Y. Hang, Enhanced emission of 2.86 μm from diode-pumped Ho^{3+}/Yb^{3+}-codoped PbF_2 crystal, Opt Express, 23(2015) 3920-3927, 10.1364/OE.23.003920

[50]Y. P. Peng, Y. Guo, J. Zhang and L. Zhang, Ho^{3+}/Yb^{3+}-codoped germanate-tellurite glasses for 2.0 μm emission performance, Appl Opt, 53(2014) 1564-1569, 10.1364/AO.53.001564

[51]Z. Xuelu and H. Toratani, Spectroscopic properties and energy transfers in Tm^{3+} singly-and Tm^{3+}/Ho^{3+} doubly-doped glasses Journal of Non-Crystalline Solids, 195(1996) 113-124, 10.1016/0022-3093(95)00522-6